Tectonophysics, 211 (1992) 305–316
Elsevier Science Publishers B.V., Amsterdam

Relationships between sliding behavior and internal geometry of laboratory fault zones and some creeping and locked strike-slip faults of California

D.E. Moore and J. Byerlee

U.S. Geological Survey, MS/977, Menlo Park, CA 94025, USA

(Received January 16, 1991; revised version accepted September 13, 1991)

ABSTRACT

Moore, D.E. and Byerlee, J., 1992. Relationships between sliding behavior and internal geometry of laboratory fault zones and some creeping and locked strike-slip faults of California. In: T. Mikumo, K. Aki, M. Ohnaka, L.J. Ruff and P.K.P. Spudich (Editors), Earthquake Source Physics and Earthquake Precursors. *Tectonophysics*, 211: 305–316.

In order to relate fault geometries to sliding behavior, maps of recently active breaks within the Hayward fault of central California, which is characterized by fault creep, have been examined and compared to maps of the San Andreas fault. The patterns of recent breaks of the Hayward fault are consistent with those found within the creeping section of the San Andreas, and they appear to have plausible physical explanations in the findings of laboratory experiments. The distinguishing geometric features of the examined locked and creeping faults are: (1) P-type second-order traces predominate over R(Riedel)-type traces in creeping sections; and (2) R-type second-order traces make smaller angles to the local fault strike in creeping sections than they do in locked sections. Two different maps of the Hayward fault gave similar results, supporting the inference that the patterns identified are basic characteristics of the fault rather than artifacts of a particular mapping procedure.

P shears predominate over R shears under laboratory conditions that allow dilation within the fault zone. In our own experiments, P-shear development was favored by the generation of excess pore-fluid pressures. We propose that creep in California faults also is the result of fluid overpressures that are maintained in a low-permeability gouge zone and that significantly lower effective stresses, thus helping to stabilize slip and producing high values of the ratio P/R. Small R-trace angles may also be an indicator of low effective stresses, but the evidence for this is not conclusive because other factors can also affect the size of the angles.

Introduction

Fault creep was first identified in 1960 along part of the San Andreas fault zone (Steinbrugge and Zacher, 1960; Tocher, 1960). Since then, creep has been documented on the Hayward and Calaveras faults of northern California (Fig. 1) (e.g., Bolt and Marion, 1966; Bonilla, 1966; Cluff and Steinbrugge, 1966; Pope et al., 1966; Radbruch, 1968), and possible examples have also been reported from a few other faults in California (e.g., Allen, 1968; Proctor, 1974; Cohn et al., 1982) and Turkey (e.g., Aytun, 1982). Why some faults or sections of faults exhibit creep while others are locked, remains a major question that we are addressing through the combined study of the geometry of some California faults and the shear patterns produced in layers of gouge during triaxial friction experiments. The main purpose of this research is to identify any physical differences between creeping (stable) and locked (stick-slip) faults that can be used to understand the controls on sliding behavior. An additional benefit is that any distinguishing characteristics that are found could potentially be used to evaluate the seismic potential of other faults.

Correspondence to: D.E. Moore, U.S. Geological Survey, MS/977, Menlo Park, CA 94025, USA.

Our initial efforts were concentrated on the laboratory samples and the San Andreas fault zone. We examined thin sections of several different types of fault gouge from triaxial friction experiments that were run under a wide range of conditions, to produce many examples each of stable and stick-slip displacement (Moore et al., 1986, 1989). U.S.G.S. maps of recently active breaks within the San Andreas fault zone (Ross, 1969; Brown, 1970, 1972; Vedder and Wallace, 1970; Brown and Wolfe, 1972; Sarna-Wojcicki et al., 1975) were the sources of fault-trace data for the investigation of natural fault patterns (Moore and Byerlee, 1991). Each study yielded a distinguishing geometric feature:

(a) (Laboratory) The maximum angle that R-type traces (Fig. 2) make with the boundary of the gouge layer (Riedel angle) is larger in samples from stick-slip experiments than in the ones from stable-slip experiments.

(b) (San Andreas) P-type fault traces (Fig. 2) predominate over R-type traces in the creeping section of the San Andreas fault, whereas the opposite relation holds in the locked sections.

The correlation between the Riedel angles and sliding behavior identified in the laboratory samples was also found in the San Andreas study. However, the variations in P/R ratio with sliding behavior along the San Andreas were only partly consistent with the examined laboratory faults. A small number of samples contained numerous P shears, and the R-shear orientations and sliding behavior of all of those samples were analogous to the creeping section. Nevertheless, R shears predominate over P shears in the great majority of our stick-slip and stably sliding samples. This

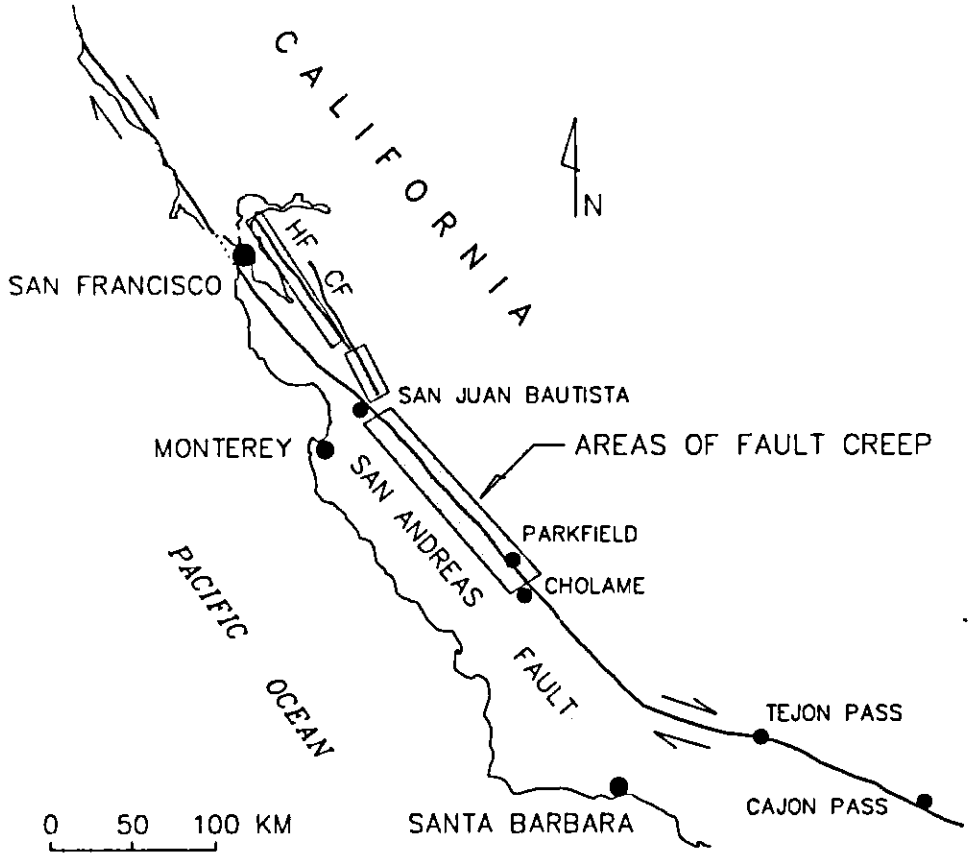

Fig. 1. Localities of faults in California that are mentioned in this study: *HF* = Hayward fault; *CF* = Calaveras fault. The stippled pattern indicates sections of these faults that are characterized by creep.

apparently weak correlation can be explained in one of two ways: first, the abundance of P traces in the creeping section of the San Andreas could be a product of the local lithology, structure, or other factor unrelated to the sliding behavior; second, the experimental conditions considered might be inappropriate for application to natural faults. The purposes of the present study were: (1) to test the validity of the San Andreas results, in particular the relative proportions of P and R traces, through the examination of other fault maps; and (2) to seek a physical explanation for the observed fault patterns.

Analysis of Hayward fault

The right-lateral Hayward fault of central California (Fig. 1) has been mapped by Radbruch-Hall (1974) and Herd (1977, 1978). Both maps cover a 75-km stretch on the northern end of the fault that contains the known areas of creep. Southeast of the mapped section, strike-slip faulting is replaced by thrust and high-angle reverse faults. The two map versions were examined separately and the results compared, in order to determine the effects of mapping style on the observed fault patterns. Consideration of the Hayward fault provides a check on the anomalous P/R ratios observed in the creeping section of the San Andreas fault. The southern part of the Calaveras fault (Fig. 1) also exhibits fault creep; indeed, the Hayward fault and the creeping sections of the Calaveras and San Andreas faults form a more or less continuous zone of creep. The Calaveras fault was not included in this study, however, because some of the recent breaks within the more obliquely oriented segments of that fault may have vertical as well as horizontal offsets, which would complicate the fault patterns.

The examined maps of the Hayward fault show the disposition of recently active fault traces, which were identified by geomorphic features

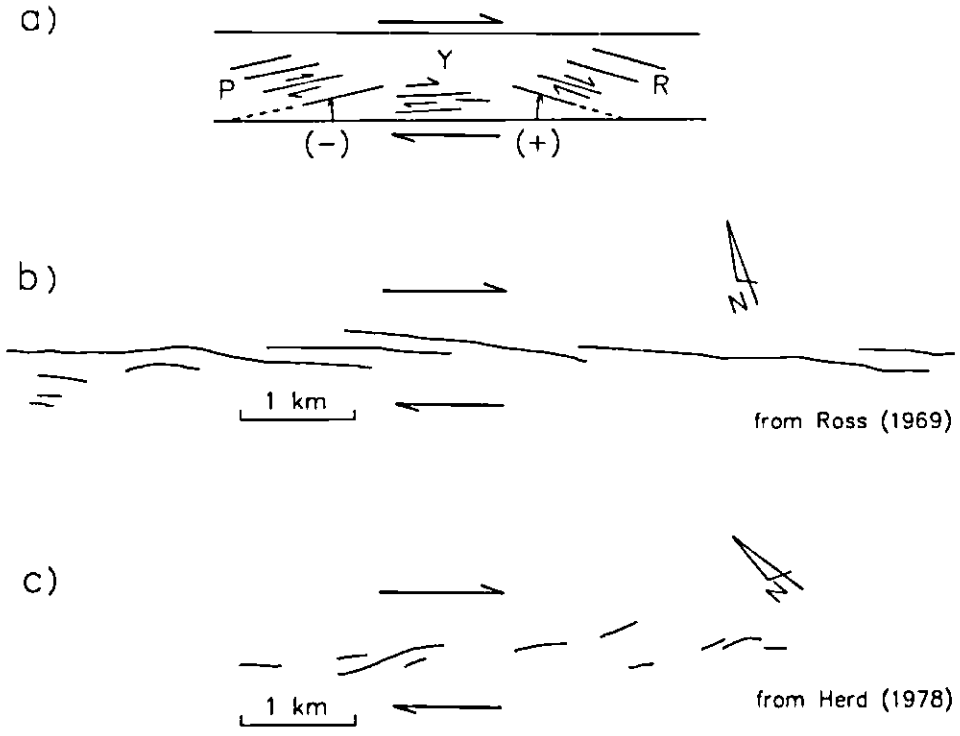

Fig. 2. (a) Labelling scheme and sign convention for selected second-order shears found in laboratory and natural fault zones. The R, P, and Y traces shown have the same sense of offset as that of the fault zone. (b) A section of the San Andreas fault, located about 20 km southeast of Tejon Pass, which contains predominantly left-stepping, R-type traces, as mapped by Ross (1969). (c) A section of the Hayward fault, located in the foothills east of Oakland, California, which contains principally right-stepping, P-type traces, as mapped by Herd (1978).

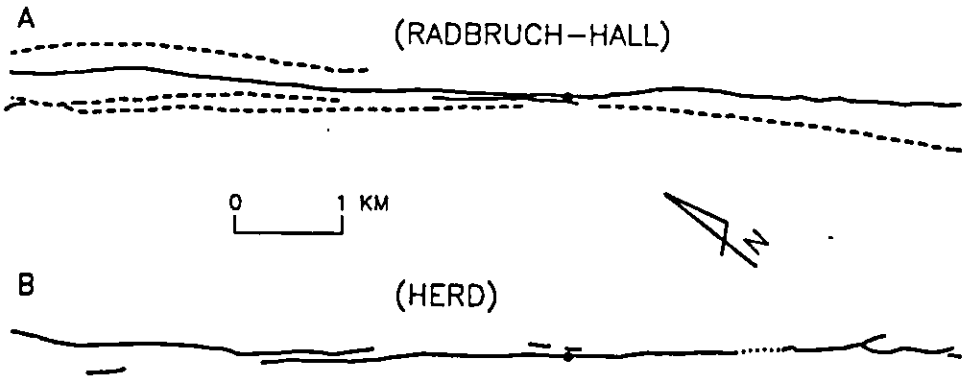

Fig. 3. Maps of recently active breaks along the same 9.5-km-long stretch of the Hayward fault passing through the city of Hayward, traced from (A) Radbruch-Hall (1974) and (B) Herd (1978). The dot on each map marks the site of the Hayward city hall.

such as scarps, trenches, offset streams, sag ponds, and lines of springs or trees. The maps were prepared by a combination of field and aerial-photograph examinations (procedures are outlined in the text to each map). Many of the criteria for recent movement are ephemeral features, and their degree of preservation varies with climatic conditions, the rate of sedimentation or erosion, and the amount of human activity. Relative to this study, the Hayward fault is located in a highly urbanized area, on the west side of a range of hills that are subject to extensive landsliding. As a result, the evidence for many recent breaks may have been lost beneath landslides, buildings, and roads. Some fault traces were identified from old aerial photographs that predated construction.

The mapping styles of Radbruch-Hall (1974) and Herd (1977, 1978) differ, as illustrated in Figure 3. Radbruch-Hall drew long, continuous fault traces (Fig. 3A), and she included some possibly older, inactive traces obtained from other

TABLE 1

Measurements of R, P, and Y traces in some California faults

	Hayward fault		San Andreas fault [a]	
	Radbruch-Hall	Herd	creeping section	locked sections
Total measured length of recent breaks, L (km)	181.5	84.4	205.9	1123.4
Case 1: Range of Y-trace orientations = $-1°$ to $+1°$				
R (km)	52.3	31.8	66.7	536.1
Y (km)	51.8	14.9	49.7	236.7
P (km)	77.5	37.7	89.4	350.7
P/R	1.48	1.19	1.34	0.65
Y/L	0.29	0.18	0.24	0.21
Case 2: Range of Y-trace orientations = $-4°$ to $+4°$				
R (km)	35.2	16.7	39.4	359.1
Y (km)	103.7	38.1	112.5	544.6
P (km)	42.6	29.7	53.9	220.7
P/R	1.21	1.78	1.37	0.61
Y/L	0.57	0.45	0.55	0.48

[a] From Moore and Byerlee (1991).

map sources. The recent breaks mapped by Herd tend to be shorter, producing a discontinuous pattern (Figs. 2c, 3B). He also mapped numerous landslides that cover the fault zone and generally did not connect fault traces across them. As a result, Radbruch-Hall's map contains more than twice the length of fault traces than are found on Herd's map (Table 1).

For each map version, the orientations of the recently active breaks were measured relative to the local strike of the fault zone. The procedures are described in detail in Moore and Byerlee (1991) and outlined briefly below. Because the trend of any fault zone will vary along its length, the fault was divided into segments of uniform strike bounded by geometric discontinuities such as bends or stepovers (Barka and Kadinsky-Cade, 1988; Knuepfer, 1989). The average trend (strike) line for a given segment was drawn as closely as possible to the main trace of the fault zone, and segment boundaries were placed, where possible, at marked changes in the faulting pattern. The strikes and lengths of all the recent breaks within each segment were then measured. As with the fault zone as a whole, the individual traces are seldom straight lines. For the most part, curved traces were divided into smaller lengths of relatively uniform trend, because the longer breaks may have formed through the linkage of shorter, en echelon traces whose orientations are of primary interest to this study. However, the average orientation of a given curved trace was reported if the variations in fault-line orientations clearly were caused by the effects of topography on the position of the fault trace. Both subdividing and averaging are subjective processes, and the re-

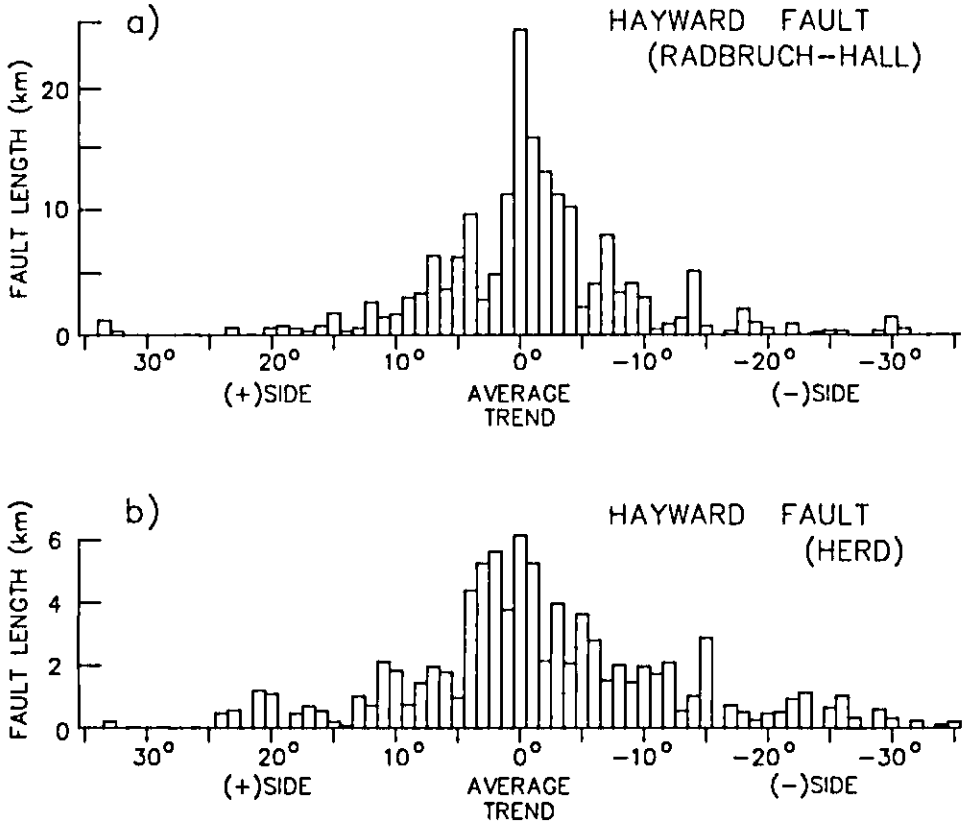

Fig. 4. Histograms of the lengths of recently active breaks relative to the average trend (local fault strike) for the Hayward fault, with data in (a) obtained from Radbruch-Hall (1974) and that in (b) from Herd (1977, 1978). The designations of positive and negative angles are as shown in Figure 2: R traces make positive angles to the strike of the fault zone and P traces make negative angles.

ported fault lengths and orientations are to be considered in a comparative rather than an absolute sense.

Although the study of fault segmentation has gained considerable attention in recent years (e.g., Segall and Pollard, 1980; Schwartz and Sibson, 1989), the focus of this report is not on the characteristics of the individual segments. Instead, the orientations of recent breaks within each segment were normalized by setting the average trend of the segment to 0° and adopting the sign convention for fault angles that is illustrated in Figure 2. In this way, the fault-length and -orientation data from different segments could be grouped together for overall consideration of the fault zone.

Results

Despite the different mapping styles of the investigators (i.e., Radbruch-Hall and Herd) (Fig. 3), the two map versions of the Hayward fault yielded very similar segment configurations. Nine segments averaging about 8 km in length were obtained from Radbruch-Hall's map and 8 segments averaging 9.4 km in length were defined from Herd's map. Equivalent segment boundaries on the two maps generally were located within a few hundred meters of each other. The strikes of comparable segments also were very close. The principal differences in segmentation occur in a complex area just northwest of the stretch of faulting depicted in Figure 3.

Histograms of the lengths of recent breaks from both maps relative to their orientations about the local average trend are presented in Figure 4. The ±35° limits were chosen because they represent the maximum R- and P-shear angles found in laboratory fault zones (Moore et al., 1988). Less than 500 m of fault length falls outside the angular limits of either histogram. On both plots, the mode of fault length coincides with the local strike, although the histogram derived from Radbruch-Hall's map has a larger peak at 0°. Both histograms are truncated on the positive-angle (R) side, both of them essentially terminating at +23 to +24°, although small lengths of fault are encountered on both histograms beyond an 8° gap on the R-trace side. On the negative-angle (P) side, the fault length tapers off gradually, without a significant gap, to angles larger than −30°. Both histograms are also skewed towards the negative-angle side, indicating that more P than R traces are present; ratios of P/R for various angular ranges of R, P, and Y traces are presented in Table 1.

Another way to estimate the relative proportions of R and P traces is to consider the arrangement of the recent breaks in the fault zone. Within the right-lateral Hayward fault, an echelon array of P traces would be right-stepping whereas an echelon array of R traces would be left-stepping (Fig. 2). To the extent that the recent breaks are arranged en echelon, counts of left and right steps between the mapped traces should give an indication of the relative abundances of R- and P-type breaks, and the results will be independent of both the choice of segments and the measurements of fault-trace orientations. Stepover counts were made by following a principal slip path along the fault zone. Because some junctures could be counted in more than one way, the stepover counts are reported as ranges of numbers that reflect the different choices possible.

The total numbers of stepovers in the two maps of the Hayward fault differ because of the differences in mapping styles described above, but the relative abundances of left and right steps are the same. Depending on the choice of principal slip path, 3–4 right steps and 2 left steps were counted on Radbruch-Hall's map, whereas 12–19 right steps and 5–6 left steps were counted on Herd's map. In both cases, right stepovers outnumber left stepovers, consistent with the presence of more P than R traces on the Hayward fault. The arrangement of fault traces in several portions of Herd's map is clearly that of right-stepping, P-type en echelon breaks (Figs. 2c, 3B). Although the Calaveras fault was not analyzed for this study, some reports are suggestive that its recently active breaks may be arranged similarly to those of the Hayward fault. For example, according to Armstrong et al. (1980), traces displaying right-lateral creep near San Felipe Lake on

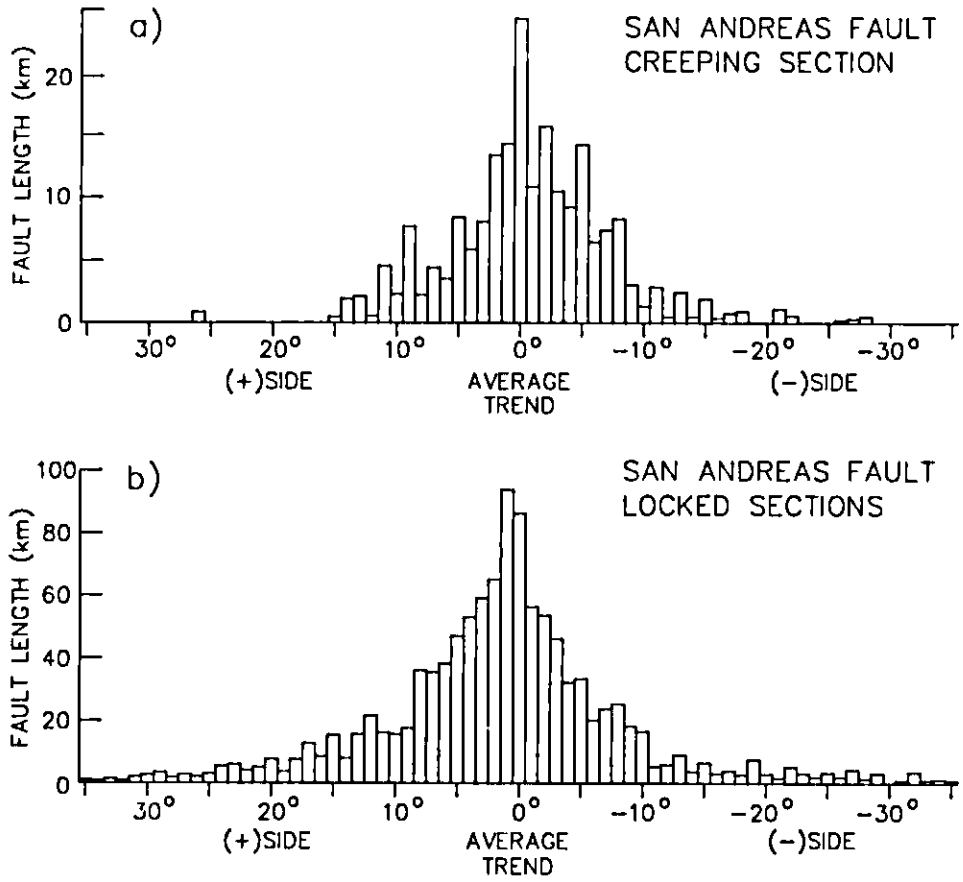

Fig. 5. Histograms of the lengths of recently active breaks relative to the local average trend for the San Andreas fault: (a) creeping section; (b) locked sections.

the Calaveras fault occur as right-stepping (P-type) en echelon strands.

Discussion

Comparison with San Andreas results

The overall patterns of recent breaks in the Hayward fault are consistent with the results described previously by Moore and Byerlee (1991) for the creeping section of the San Andreas fault zone. The ratio P/R is greater than 1 for both the Hayward fault and the creeping section of the San Andreas (Table 1), and the histograms of these corresponding fault sections have the same truncated appearance (Figs. 4, 5a). The proportions of P and R traces and Riedel angles in the Hayward fault are readily distinguished from locked sections of the San Andreas (Table 1; Figs. 4, 5). The relative abundances and orientations of secondary traces within both fault zones may therefore be generally correlated with their mode of slip.

One difference between the Hayward fault and the creeping section of the San Andreas fault is in the size of the maximum Riedel angle. Although the R-trace sides of the histograms of the Hayward fault are truncated, the maximum angle is 8° to 10° larger than that measured for the San Andreas creeping section. The larger angles may be associated with the relative youth of the Hayward fault compared to the San Andreas, because faults tend to acquire smaller-angle second-order traces as they mature (Morgenstern and Tchalenko, 1967; Tchalenko, 1970; Mandl et al., 1977). Moore et al. (1988) also found that the mineralogy of the gouge affects the Riedel angle to some extent, although the

only significant difference is that larger Riedel angles are associated with a gouge composed of pure quartz sand. The other gouges tested, including illite- and montmorillonite-rich gouges, crushed granite, and serpentine, all had similar Riedel angles. Thus, mineralogy probably has no effect on Riedel shear orientations in the Hayward fault.

Similar fault patterns were identified from two superficially disparate maps of the Hayward fault. Close positioning of segment boundaries and similar P/R ratios and Riedel angles were also found for two maps of the western Big Bend section of the San Andreas fault prepared by Vedder and Wallace (1970) and Davis and Duebendorfer (1987). This suggests that geometric discontinuities and the arrangement of recent breaks are basic features of fault zones that can be identified despite stylistic differences in their depiction. The two maps of the Hayward fault also gave comparable results despite the inclusion of older, possibly inactive traces in the one prepared by Radbruch-Hall (1974). If fault geometry is a good indicator of sliding behavior, then the Hayward fault may also have exhibited creep back to the time that the older traces were active.

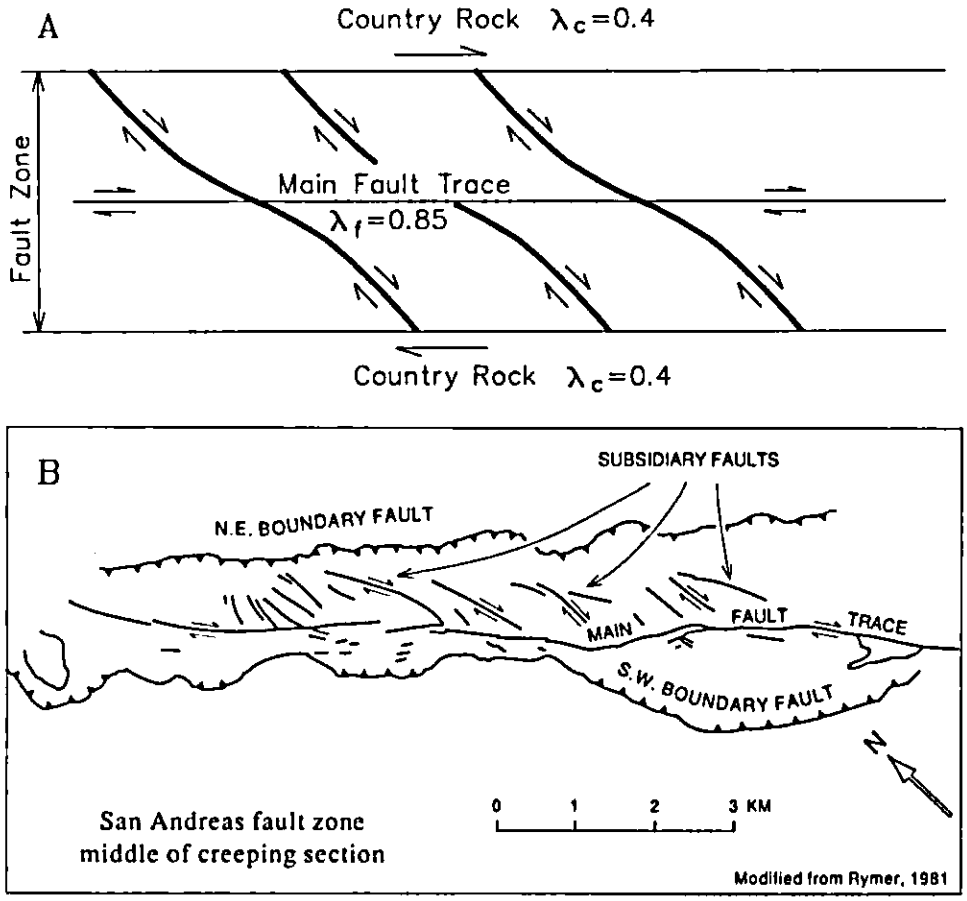

Fig. 6. Comparison of model and natural fault-zone configurations. (A) Schematic diagram of a fault zone containing material with a threshold gradient that results in a pore pressure of 85% of the lithostatic stress on the main fault trace; taken from figure 5 of Byerlee (1992, this volume). The maximum principal stress measured on the flanks of the fault is oriented at about 80° to the fault, and failure in the outer zones occurs at the orientations shown by the curved traces. (B) Map of boundary faults and recently active breaks within a portion of the creeping section of the San Andreas fault; modified by M. Rymer from his (1981) map (see also fig. 3 of Rymer et al., 1984). The subsidiary fractures mapped by Rymer correspond to the large-angle breaks in the outer zones of the model fault in (A); the main trace consists predominantly of right-stepping (P-type) recent breaks.

P/R ratios

A hypothesis for the generation of high P/R ratios has been suggested by Gamond (1983) that may explain the apparently minimal correlation between the field and laboratory results. The experiments of Gamond (1983) illustrate conditions under which P shears can predominate along a given section of fault. Gamond demonstrated that if direct-shear experiments are carried out on clay at a sufficiently low, constant normal stress, then dilation within the fault zone is possible. During the experiments, R shears formed first, consistent with other laboratory samples deformed in simple shear. The establishment of the R shears causes changes in the stress fields in the intervening areas, which leads to the formation of P shears at those sites. As illustrated in Figure 2, the stepover zone between adjacent R shears is compressional, whereas that between adjacent P shears is dilational. In a compressional regime, offset along the R shears would be favored. However, because of the low fault-normal stresses of Gamond's experiments, the secondary P shears became the locus of slip and the primary R traces opened passively to form prismatic depressions.

By analogy to the laboratory faults examined by Gamond (1983), we suggest that effective stresses acting on the creeping sections of the San Andreas and Hayward faults are lower than in the locked sections. The differences are such that dilation within creeping faults is possible, and P traces become the locus of shear with continued offset over time. In locked faults, which are subject to higher effective stresses, the R traces predominate and the P traces are relegated to minor, connecting structures. In our laboratory studies on illite gouge (Moore et al., 1989), the samples containing many P shears were ones in which large fluid overpressures appear to have been generated accompanying heating. Heating also caused the gouge layers to become lithified, which reduced their permeability and increased the amount of time required to alleviate the excess pressures. The overpressured samples had lower strength and greater sliding stability than equivalent, equilibrated samples. From comparison with our laboratory results, we propose that high pore pressures maintained in a low-permeability, sheet-silicate-rich gouge are responsible for the low effective stresses of the creeping zones.

The association of fault creep with high pore pressures is not a new idea (e.g., Byerlee and Brace, 1972; Berry, 1973; Irwin and Barnes, 1975), but Byerlee (1992, this volume) has only recently demonstrated how fluid overpressures can be maintained within a fault zone. Byerlee proposed that the presence of low-permeability, clay-rich gouge within the fault zone leads to the development of excess fluid pressures. At very low pressure gradients, water will not flow through dense clay. A gouge zone of sufficient width can maintain near-lithostatic pore pressures at its center, even though hydrostatic pressures exist at the gouge–country rock boundary (Fig. 6A). Thus, whatever stresses exist exterior to the fault zone, the center of the fault can be extremely weak. Within this central zone, the maximum principal stress is oriented at 45° to the strike of the fault, consistent with models of simple shear (Byerlee, 1992, this volume). In the country rock adjoining the fault, the maximum principal stress is oriented at a high angle to the fault strike (Byerlee, 1992, this volume).

Within the creeping section of the San Andreas fault, Rymer (1981; see also Rymer et al., 1984) mapped an approximately 2-km wide fault zone consisting of a central zone (main trace) containing predominantly right-stepping (P) breaks that are oriented at small angles to the local strike of the fault, and outer zones containing active, subsidiary breaks that make substantially larger angles to the local strike of the San Andreas (Fig. 6B). The main trace of Rymer (1981) corresponds to the zone of recently active breaks that was mapped by Brown (1970) and also to the central zone of very low effective stress of the model fault of Byerlee (1992, this volume) (Fig. 6A). The orientation of the large-scale subsidiary faults northeast of the main trace is consistent with an orientation of the maximum principal stress nearly perpendicular to the strike of the San Andreas, similar to the model fault of Figure 6A.

Byerlee's (1992, this volume) model explains nearly fault-normal compression, which has also

been reported in locked sections of the San Andreas fault (e.g., Mount and Suppe, 1987; Zoback et al., 1987). Byerlee suggested, however, that his model is most likely to be applicable to the sections showing fault creep. As illustrated in Figure 6, fault-zone configurations consistent with his model are found in areas of fault creep. A difference in the width of the gouge zone contained in locked and creeping sections could account for the differences in sliding behavior (Byerlee, 1990). A narrower gouge zone would lower the maximum fluid pressure attainable at its center and in turn raise the effective stresses acting on the fault. Relative to this idea, Rymer (1982) reported that low-density serpentine from altered ultramafic rocks at the base of the Franciscan Complex has been injected into part of the San Andreas creeping section. The addition of serpentine to the fault would increase the width of sheet-silicate-rich fault gouge, which in turn would help to maintain high fluid pressures along the main trace. The other major occurrences of fault creep in California have a geological setting similar to that mapped by Rymer (1981, 1982); the structural sequence consists of the basal Franciscan Complex, capped in turn by the Coast Range ophiolite and the Great Valley Sequence. Serpentine from the Franciscan Complex or the Coast Range ophiolite could have been injected into these faults as well (e.g., Irwin and Barnes, 1975), to add to the width of the central zone.

As figured in Wallace (1973), a few local concentrations of P traces are found in the locked sections of the San Andreas (see also Moore and Byerlee, 1989). Such occurrences might possibly reflect the local development of high pore-fluid pressures, and they should be examined for evidence of fault creep. It is possible, though, that a greater length of fault is required to initiate fault creep than is available in these segments.

Riedel angles

As described previously (Moore et al., 1989; Moore and Byerlee, 1991), the observed Riedel angles are not readily interpreted using Coulomb theory. However, the explanation put forward for the P/R ratios suggests a way to identify the physical controls on the Riedel angles, even though the underlying mechanics remain obscure. For our experiments with the illite-rich gouge (Moore et al., 1989), the size of the Riedel angle was specifically correlated with the sliding behavior, such that small Riedel angles were associated with stable slip and large Riedel angles with stick slip. In addition, those stick-slip samples with the largest stress drops also had the largest measured Riedel angles. Changes in any parameter that controls sliding behavior will therefore affect the R-shear orientations. With respect to the experiments using the illite-rich gouge, stick-slip motion and large Riedel angles were favored by increases in temperature and effective pressure and decreases in sliding velocity. Those P-shear-rich samples with large fluid overpressures were characterized by reduced strength, more stable motion, and smaller-angle R-shear orientations than associated, equilibrated samples. Gamond (1983) also found that in undrained samples the Riedel angles decreased with decreasing normal stress. If, as described above, high pore-fluid pressures are responsible for the occurrence of fault creep in parts of the San Andreas, Hayward, and Calaveras faults, then they should also be responsible for the lower Riedel angles measured in the sections with fault creep.

Temperature and velocity variations, which influenced sliding behavior in our experiments (Moore et al., 1989), can probably be discounted as controls on R-trace orientations in the examined California faults. For one thing, each laboratory experiment was conducted at a single temperature, whereas a fault in the earth's crust is subjected to increasing temperature with depth. Variations in the temperature profile will affect the vertical extent of the seismogenic zone (e.g., Sibson, 1982), not the occurrence or lack of occurrence of fault creep within the seismogenic zone. The rates of offset along the various examined faults also have no correlation with sliding behavior. Thus, both the orientations of the R traces and their abundances relative to P traces are, at present, best explained as being controlled by fluid pressure.

Future studies

The model proposed in this paper can be tested by means of both field and laboratory studies. The most direct test would be to measure pore-fluid pressures at depth within creeping and locked sections of the faults, to determine whether the fault patterns are correlated with pore pressures. Measurements of pore pressure should also be made at various positions between the main trace and outer boundaries of the fault zones, to test for the presence of a pore-pressure gradient across the faults. In the laboratory, we shall be conducting triaxial experiments at combined high pore pressures and low effective pressures, to see if we can generate the high P/R ratios observed in creeping faults. Sliding experiments involving a wide clay layer subjected to a gradient in pore pressure are also being planned.

Conclusions

The results of this study are consistent with previous work, which suggests that the internal geometry of creeping (stable slip) faults differs from that of locked (stick slip) faults. The faulting patterns are sufficiently robust that they are not obscured by the mapping style adopted. The high P/R ratios and possibly also the small Riedel angles of creeping zones may be indicators of near-lithostatic fluid pressures within the faults, which lower the effective stresses sufficiently to allow stable slip to occur. The high effective stresses used in most triaxial friction experiments may be inappropriate for the characterization of creep in natural faults.

References

Allen, C.R., 1968. The tectonic environments of seismically active and inactive areas along the San Andreas fault system. In: W.R. Dickinson and A. Grantz (Editors), Proc. Conf. Geologic Problems of San Andreas Fault System. Stanford Univ. Publ. Geol. Sci., 11: 70–80.

Armstrong, C.F., Wagner, D.L. and Bortugno, E.J., 1980. Movement along the southern Calaveras fault zone as shown by fence line surveys. In: R. Streitz and R. Sherburne (Editors), Studies of the San Andreas Fault Zone in Northern California. Calif., Div. Mines Geol., Spec. Rep., 140: 29–39.

Aytun, A., 1982. Creep measurements in the Ismetpasa region of the North Anatolian fault zone. In: A.M. Isikara and A. Vogel (Editors), Multidisciplinary Approach to Earthquake Prediction. Vieweg, Braunschweig, pp. 279–295.

Barka, A.A. and Kadinsky-Cade, K., 1988. Strike-slip fault geometry in Turkey and its influence on earthquake activity. Tectonics, 7: 663–684.

Berry, F.A.F., 1973. High fluid potentials in California Coast Ranges and their tectonic significance. Am. Assoc. Pet. Geol. Bull., 57: 1219–1249.

Bolt, B.A. and Marion, W.C., 1966. Instrumental measurements of slippage on the Hayward fault. Bull. Seismol. Soc. Am., 56: 305–316.

Bonilla, M.G., 1966. Deformation of railroad tracks by slippage on the Hayward fault in the Niles district of Fremont, California. Bull. Seismol. Soc. Am., 56: 281–289.

Brown, R.D., Jr., 1970. Map showing recently active breaks along the San Andreas and related faults between the northern Gabilan Range and Cholame Valley, California. U.S. Geol. Surv. Misc. Geol. Invest. Map I-575, scale 1:62,500.

Brown, R.D., Jr., 1972. Active faults, probable active faults, and associated fracture zones, San Mateo County, California. U.S. Geol. Surv. Misc. Field Stud. Map MF-355, scale 1:62,500.

Brown, R.D., Jr. and Wolfe, E.D., 1972. Map showing recently active breaks along the San Andreas fault between Point Delgada and Bolinas Bay, California. U.S. Geol. Surv. Misc. Geol. Invest. Map I-692, scale 1:24,000.

Byerlee, J., 1990. Friction, overpressure, and fault normal compression. Geophys. Res. Lett., 17: 2109–2112.

Byerlee, J., 1992. The change in orientation of subsidiary shears near faults containing high pore fluid pressure. In: T. Mikumo, K. Aki, M. Ohnaka, L.J. Ruff and P.K.P. Spudich (Editors), Earthquake Source Physics and Earthquake Precursors. Tectonophysics, 211: 295–303.

Byerlee, J.D. and Brace, W.F., 1972. Fault stability and pore pressure. Bull. Seismol. Soc. Am., 62: 657–660.

Cluff, L.S. and Steinbrugge, K.V., 1966. Hayward fault slippage in the Irvington–Niles districts of Fremont, California. Bull. Seismol. Soc. Am., 56: 257–279.

Cohn, S.N., Allen, C.R., Gilman, R. and Goulty, N.R., 1982. Preearthquake and postearthquake creep on the Imperial fault and the Brawley fault zone. In: The Imperial Valley, California, Earthquake of October 15, 1979. U.S. Geol. Surv. Prof. Pap. 1254: 161–167.

Davis, T.L. and Duebendorfer, E.M., 1987. Strip map of the western big bend segment of the San Andreas fault. Geol. Soc. Am. Map Chart Ser. Map MC-60, scale 1:31,682.

Gamond, J.F., 1983. Displacement features associated with fault zones: a comparison between observed examples and experimental models. J. Struct. Geol., 5: 33–45.

Herd, D.G., 1977. Map of Quaternary faulting along the

Hayward and Calaveras fault zones. U.S. Geol. Surv. Open-File Map 77-645, scale 1:24,000.

Herd, D.G., 1978. Map of Quaternary faulting along the northern Hayward fault zone. U.S. Geol. Surv. Open-File Rep. 78-308, scale 1:24,000.

Irwin, W.P. and Barnes, I., 1975. Effect of geologic structure and metamorphic fluids on seismic behavior of the San Andreas fault system in central and northern California. Geology, 3: 713-716.

Knuepfer, P.L.K., 1989. Implications of the characteristics of end-points of historical surface fault ruptures for the nature of fault segmentation. In: D.P. Schwartz and R.H. Sibson (Editors), Fault Segmentation and Controls of Rupture Initiation and Termination. U.S. Geol. Surv. Open-File Rep. 89-315: 193-228.

Mandl, G., de Jong, L.N.J. and Maltha, A., 1977. Shear zones in granular material: an experimental study of their structure and mechanical genesis. Rock Mech., 9: 95-144.

Moore, D.E. and Byerlee, J., 1989. Geometry of recently active breaks along the San Andreas fault, California. U.S. Geol. Surv. Open-File Rep. 89-347, 72 pp.

Moore, D.E. and Byerlee, J.D., 1991. Comparative geometry of the San Andreas fault, California, and laboratory fault zones. Geol. Soc. Am. Bull., 103: 762-774.

Moore, D.E., Summers, R. and Byerlee, J.D., 1986. The effects of sliding velocity on the frictional and physical properties of heated fault gouge. Pure Appl. Geophys., 124: 31-52.

Moore, D.E., Summers, R. and Byerlee, J.D., 1988. Relationship between textures and sliding motion of experimentally deformed fault gouge: Application to fault zone behavior. In: P.A. Cundall, R.L. Sterling and A.M. Starfield (Editors), Key Questions in Rock Mechanics. Proc. U.S. Symp. Rock Mechanics, 29th, pp. 103-110.

Moore, D.E., Summers, R. and Byerlee, J.D., 1989. Sliding behavior and deformation textures of heated illite gouge. J. Struct. Geol., 11: 329-342.

Morgenstern, N.R. and Tchalenko, J.S., 1967. Microscopic structures in kaolin subjected to direct shear. Géotechnique, 17: 309-328.

Mount, V.S. and Suppe, J., 1987. State of stress near the San Andreas fault: implications for wrench tectonics. Geology, 15: 1143-1146.

Pope, A.J., Stearn, J.L. and Whitten, C.A., 1966. Surveys for crustal movement along the Hayward fault. Bull. Seismol. Soc. Am., 56: 317-323.

Proctor, R.J., 1974. New localities for fault creep in southern California—Raymond and Casa Loma faults. Geol. Soc. Am. Abstr. Progr., 6: 238.

Radbruch, D.H., 1968. New evidence of historic fault activity in Alameda, Contra Costa, and Santa Clara Counties, California. In: W.R. Dickinson and A. Grantz (Editors), Proc. Conf. Geologic Problems of San Andreas Fault System. Stanford Univ. Publ. Geol. Sci., 11: 46-54.

Radbruch-Hall, D.H., 1974. Map showing recently active breaks along the Hayward fault zone and the southern part of the Calaveras fault zone, California. U.S. Geol. Surv. Misc. Invest. Ser. Map I-813, scale 1:24,000.

Ross, D.C., 1969. Map showing recently active breaks along the San Andreas fault between Tejon Pass and Cajon Pass, southern California. U.S. Geol. Surv. Misc. Invest. Ser. Map I-553, scale 1:24,000.

Rymer, M.J., 1981. Geologic map along a 12 kilometer segment of the San Andreas fault zone, southern Diablo Range, California. U.S. Geol. Surv. Open-File Rep. 81-1173, scale 1:12,000.

Rymer, M.J., 1982. Structural framework of the San Andreas fault zone along Mustang Ridge, Monterey County, California. Geol. Soc. Am. Abstr. Progr., 14: 229.

Rymer, M.J., Lisowski, M. and Burford, R.O., 1984. Structural explanation for low creep rates on the San Andreas fault near Monarch Peak, central California. Bull. Seismol. Soc. Am., 74: 925-931.

Sarna-Wojcicki, A.M., Pampeyan, E.H. and Hall, N.T., 1975. Map showing recently active breaks along the San Andreas fault between the central Santa Cruz Mountains and the northern Gabilan Range, California. U.S. Geol. Surv. Misc. Field Stud. Map MF-650, scale 1:24,000.

Schwartz, D.P. and Sibson, R.H. (Editors), 1989. Fault Segmentation and Controls of Rupture Initiation and Termination. U.S. Geol. Surv. Open-File Rep. 89-315, 447 pp.

Segall, P. and Pollard, D.D., 1980. Mechanics of discontinuous faults. J. Geophys. Res., 85: 4337-4350.

Sibson, R.H., 1982. Fault zone models, heat flow, and the depth distribution of earthquakes in the continental crust of the United States. Bull. Seismol. Soc. Am., 72: 151-163.

Steinbrugge, K.V. and Zacher, E.G., 1960. Creep on the San Andreas fault. Fault creep and property damage. Bull. Seismol. Soc. Am., 50: 389-396.

Tchalenko, J.S., 1970. Similarities between shear zones of different magnitudes. Geol. Soc. Am. Bull., 81: 1625-1640.

Tocher, D., 1960. Creep on the San Andreas fault. Creep rate and related measurements at Vineyard, California. Bull. Seismol. Soc. Am., 50: 396-404.

Vedder, J.G. and Wallace, R.E., 1970. Map showing recently active breaks along the San Andreas and related faults between Cholame Valley and Tejon Pass, California. U.S. Geol. Surv. Misc. Geol. Invest. Map I-574, scale 1:24,000.

Wallace, R.E., 1973. Surface fracture patterns along the San Andreas fault. In: R.L. Kovach and A. Nur (Editors), Proc. Conf. Tectonic Problems of the San Andreas Fault System. Stanford Univ. Publ. Geol. Sci., 13: 248-250.

Zoback, M.D., Zoback, M.L., Mount, V.S., Suppe, J., Eaton, J.P., Healy, J.H., Oppenheimer, D., Reasenberg, P., Jones, L., Raleigh, C.B., Wong, I.G., Scotti, O. and Wentworth, C., 1987. New evidence on the state of stress of the San Andreas fault system. Science, 238: 1105-1111.